



Published in final edited form as:

Kidney Int. 2008 October ; 74(7): 879–889. doi:10.1038/ki.2008.304.

Kidney-derived mesenchymal stem cells contribute to vasculogenesis, angiogenesis and endothelial repair

Jun Chen^{1,3}, Hyeong-Cheon Park^{1,2,3}, Francesco Addabbo¹, Jie Ni¹, Edward Pelger¹, Houwei Li¹, Matthew Plotkin¹, and Michael S. Goligorsky¹

¹ Departments of Medicine and Pharmacology, New York Medical College, Valhalla, New York, USA

² Department of Internal Medicine, College of Medicine, Yonsei University, Seoul, Korea

Abstract

We isolated a clonal cell line (4E) from kidneys of mice expressing green fluorescent protein controlled by the endothelial-specific Tie2 promoter. When grown in a three-dimensional matrigel matrix they formed a fluorescent capillary network. *In vivo* angiogenesis assays using growth factor-depleted matrigel implanted plugs promoted a moderate angiogenesis of host endothelial cells. Using vascular endothelial growth factor (VEGF)-A and fibroblast growth factor-2 in the plugs containing 4E-cells resulted in a robust vasculogenesis. Transplantation of 4E cells into mice with acute renal ischemia showed selective engraftment in the ischemic kidney which promoted tubular regeneration by increasing epithelial proliferation and inhibiting apoptosis. This resulted in an accelerated functional recovery 3 days after ischemia. These mice showed a 5-fold increase in tissue VEGF expression compared to controls, but no difference in plasma VEGF level corresponding with better preservation of peritubular capillaries, perhaps due to a local paracrine effect following systemic 4E infusion. One month after ischemia, 9% of engrafted 4E cells expressed green fluorescent protein in the peritubular region while half of them expressed α -smooth muscle actin. Our study shows that kidney mesenchymal stem cells are capable of differentiation toward endothelial and smooth muscle cell lineages *in vitro* and *in vivo*, support new blood vessel formation in favorable conditions and promote functional recovery of an ischemic kidney.

Keywords

mesenchymal stem cells; angiogenesis; vasculogenesis; acute ischemic renal injury

Sinusoidal endothelium in bone marrow and extraosseous capillaries represent a large disseminated niche for mesenchymal stem cells (MSC), which are present, according to the recent study, in practically all postnatal organs and tissues tested.¹ This disseminated pool of MSC localized to the basement membrane of blood vessels in close contact with the vascular endothelium may be involved in the local regulation of vascular and/or tissue regeneration. Whereas osteoblastic bone marrow niche provides microenvironment supportive of stem cell quiescence, the vascular niche facilitates their proliferation, differentiation, and rapid mobilization.² These perivascular stem cells are, in part, represented by pericyte-like MSCs also termed mural stem cells.¹ MSCs have the potential to differentiate along multiple lineages

Correspondence: Jun Chen, Departments of Medicine and Pharmacology, New York Medical College, Valhalla, New York 10595, USA. jun_chen@nyc.edu or H-C Park, Department of Internal Medicine, College of Medicine, Yonsei University, Seoul, Korea. amp97@yumc.yonsei.ac.kr.

³These authors contributed equally to this work

DISCLOSURE

All the authors declared no competing interests.

in vitro, including the best characterized osteogenic, chondrogenic, and adipogenic differentiation,^{3,4} although, according to the recent data, these cells can differentiate toward endothelial cell lineage.^{5–8} The latter claim rests on the use of bone marrow-derived MSC in a canine model of chronic cardiac ischemia in which MSCs were found to be colocalized with endothelial and smooth muscle cells, but not with cardiomyocytes, 1 month after transplantation. This was associated with a trend toward reduced fibrosis and increased vascular density. Weekly injections of MSC in collagen4A3-deficient mice, a model of Alport syndrome, resulted in the reduction of renal fibrosis and prevention of the loss of peritubular capillaries in conjunction with the localization of transplanted cells in peritubular capillaries.⁹ Conflicting results demonstrating no morphologic improvement after MSC transplantation, as opposed to therapeutic efficacy of transplanting bone marrow-derived cells, in the model have been reported by Prodromidi *et al.*¹⁰ An account on the differentiation of isolated bone marrow-derived MSC cultured in a medium containing vascular endothelial growth factor into endothelial cells *in vitro* has been published by Oswald *et al.*¹¹ and Togel *et al.*¹² The apparent paucity of data on the differentiation potential of MSC toward endothelial lineage, especially *in vivo*, and the absence of published data on organ-derived MSC prompted us to investigate these issues. Our main goal was to elucidate the possible differentiation repertoire of local MSC and their contribution to tissue protection. Specifically, this study was designed to address this possibility both *in vitro* and *in vivo*. Using a clonal cell line of MSC (4E) isolated from the kidney of adult Tie-2 green fluorescent protein (GFP) transgenic FVB/NJ mice,⁸ we examined their *in vitro* and *in vivo* angiogenic and vasculogenic properties and further tested their differentiation potential in mice with acute ischemic renal injury.

RESULTS

In vitro angiogenesis

To examine the possibility that MSC can differentiate toward endothelial lineage, we tested their *in vitro* angiogenic potential using 4E cells. These cells were cloned from a single colony of the original MSC isolated from the kidney of Tie-2/GFP mice and thoroughly characterized,⁸ thus negating any contamination with endothelial cells. As illustrated in Figure 1a, when cultured on three-dimensional matrigel in EGM-2 medium, 4E cells initially formed ‘sphere’-like structures, which gradually spread out forming a dense capillary network. Some cells in these capillaries showed positive GFP signals. Fluorescence-activated cell sorter analysis of isolated capillary-forming cells cultured for 30 days indicated that about 14.8% were double positive for GFP/CD31 (under matrigel/EGM-2 medium culture conditions) as opposed to the original 4E MSC population negative for these markers (Figure 1b). When cultured in EGM-2 or MSC culture medium, 4E cells displayed scattered appearance of endothelial (Tie2-GFP) and α -smooth muscle actin (α SMA) cell markers (Figure 1c), revealing the alternative acquisition of either the endothelial or the smooth muscle cell phenotypical markers depending on the ambient conditions, namely EGM-2 or MSC medium, respectively.

In vivo neovascularization of angioreactors

We next studied the angiogenic and/or vasculogenic potential of kidney MSC (4E cells) *in vivo* using matrigel-filled implantable angioreactors (directed *in vivo* angiogenesis assay). Control angioreactors, which contained only growth factor-depleted matrigel, revealed no capillary ingrowth. Second control group, angioreactors containing growth factors only, showed a robust ingrowth of host capillaries. The 4E-containing angioreactors, within 15 days of implantation, showed an intense angiogenesis originating from the host endothelial cells and a modest vasculogenesis (Figure 2). These neovessels were apparently patent and functional, as they were stained positive for *Lycopersicon Esculentum* lectin (LEL)-FITC, administered before harvesting the subcutaneously implanted angioreactors. Considering the fact that majority of neovessels originated from the host endothelium, these results are

consistent with the paracrine signaling hypothesis.⁸ The 4E cells promoted the *in vivo* angiogenesis, presumably, through the secretion of pro-angiogenic factors and chemoattraction of the host endothelial cells.

When growth factors, vascular endothelial growth factor-A/fibroblast growth factor-2 (VEGF-A/FGF-2), were added to the 4E-containing matrigel angioreactors, a robust neovascularization occurred, in which functional (LEL-FITC-positive) vascular network was formed. We documented that the CM-DiI-labeled 4E cells were recruited into the neovasculature, when the exogenous growth factors were presented. The number of the capillary-associated 4E cells was significantly higher in the growth factor-containing group ($57.46 \pm 7.15\%$) compared with the 4E growth factor-free angioreactors ($8.54 \pm 3.01\%$) (Figure 2, inset). The high-magnification images of the neovasculature in Figure 2 (right panel) illustrate that, in the growth factor-containing matrigel, the majority of CM-DiI-labeled 4E cells recruited to the vessels were also GFP-positive, suggesting that these capillaries were formed through vasculogenesis, specifically via the differentiation of 4E cells to endothelial cells. This green fluorescent signal could be attributed to either Tie2-GFP or LEL-FITC (readily distinguishable due to the cytosolic vs luminal membrane fluorescence, respectively). However, even a potential overlap in signals would not hinder the interpretation of the results as either staining originated from endothelial cells. Furthermore, ultrathin deconvoluted fluorescent microscopy analysis confirmed that some of the cells incorporated into the neovasculature in the growth factor-containing matrigel were CM-DiI and LEL-FITC double-positive (Figure 3). Thus, in the absence of VEGF-A/FGF-2, 4E cells support angiogenesis by promoting the host endothelial cell infiltration of angioreactors, whereas in the presence of these growth factors, 4E cells transdifferentiate into endothelial cells and participate in vasculogenesis.

Transplantation of 4E cells in acute renal ischemia: transdifferentiation to endothelial or α SMA-expressing cells

Next, we addressed the possibility of 4E cell participation in vasculogenesis associated with tissue injury. Toward this end, we studied the pro-angiogenic and renoprotective potential of 4E cells using acute renal ischemia–reperfusion (I/R) model. We first examined the engraftment of the CM-DiI-labeled 4E cells in the ischemic kidney 3–30 days after transplantation (Figure 4). The number of the engrafted CM-DiI-labeled 4E cells was significantly higher in the ischemic kidney compared with the contralateral non-ischemic kidney 3 days after transplantation (1.9 ± 0.1 vs 0.2 ± 0.1 cells per mm^2 , respectively, $P < 0.01$). This difference in 4E cell engraftment to ischemic and contralateral non-clamped kidney was maintained up to 30 days (Figure 4b). Tie2-GFP signal was not detectable in kidney sections at 3–15 days after I/R injury. In contrast, by 30 days after I/R injury, $9.2 \pm 3.1\%$ of engrafted 4E cells expressed Tie2-GFP along the peritubular capillary area, suggesting a possible endothelial transdifferentiation of MSC (Figure 4c). In addition, the examination of the α SMA expression indicated that about 45 ± 6 – $55 \pm 1\%$ of the engrafted 4E cells became α SMA-positive 15–30 days after I/R injury (Figure 5).

In the next series of experiments, we examined functional consequences of 4E cell transplantation in mice with bilateral I/R injury. Thirty minutes of bilateral ischemia induced severe renal dysfunction as judged by a significant increase in plasma creatinine levels (Figure 6a): from the baseline of 0.24 ± 0.07 to 1.92 ± 0.22 mg per 100 ml 1 day after clamping. Compared with control ischemic mice, animals that received 4E cells after I/R injury had a significantly lower plasma creatinine levels 2–3 days after ischemic injury (24–48 h after cell transplantation), suggesting an early renoprotection afforded by the transplanted cells. To obtain insights into the mechanism of 4E-mediated renoprotection in I/R injury, we examined the rates of tubular epithelial cell (TEC) proliferation and apoptosis in the kidneys of control and 4E-transplanted mice. As shown in Figures 4e and 6c, transplantation significantly

increased the number of proliferating Ki-67-positive TEC (255 ± 22 vs 135 ± 16 cells per mm^2 , respectively, $P < 0.05$) and simultaneously reduced the number of apoptotic TEC on TUNEL (terminal deoxynucleotidyl transferase-mediated dUTP nick-end labeling) assay (58 ± 7 vs 117 ± 13 cells per mm^2 , respectively, $P < 0.05$). At 15 and 30 days post-ischemia, the level of plasma creatinine was similar in both groups and indistinguishable from the baseline (data not shown).

To further assess the role of 4E cells in renoprotection, microvascular density and the degree of fibrosis were examined in ischemic and control kidney sections processed for the expression of CD31 and stained with Masson's trichrome stain. As summarized in Figure 7, the degree of microvascular rarefaction was significantly reduced in 4E-transplanted vs control kidneys at early (3 days) time points after ischemia, but later these differences disappeared. Trichrome staining revealed comparable levels of fibrosis between transplanted and control post-ischemic kidneys at day 30 (1.3 ± 0.3 vs 1.6 ± 0.3 in cortex and 1.4 ± 0.3 vs 1.9 ± 0.4 in medulla, respectively). Plasma and renal tissue levels of pro- and anti-inflammatory cytokines, such as TNF- α , IL-1 α , IL- β , IL-6, KC, and IL-10, did not show significant difference between control and 4E-transplanted mice (data not shown). However, compared with control, 4E-transplanted mice showed a fivefold increase in renal tissue VEGF expression at 3 days after I/R injury (Figure 7d). In contrast, the plasma VEGF level did not show any significant difference between the two groups (9.5 ± 1.3 vs 9.4 ± 2.4 pg/ml). These data indicated that the fact that 4E cells-afforded renoprotection is, in part, due to the local VEGF paracrine effect, resulting in the preservation of peritubular capillaries, reduced apoptosis, and increased proliferation of TEC.

DISCUSSION

The focus of this study was on the potential of a kidney-derived MSC line, 4E cells previously obtained and characterized by us,⁸ to differentiate toward endothelial lineage, both *in vitro* and *in vivo*, and their contribution to organ repair after ischemic injury. Previous studies have shown that MSCs isolated mainly from the bone marrow, as well as various adult tissues, are clonogenic, plastic-adherent, multipotent cells capable of differentiating *in vitro* to a variety of cell lineages, including adipocytes, osteoblasts, chondrocytes, myoblasts, neural tissue, and endothelial cells.^{4,13–18} These unique properties have implicated MSC as promising candidates for cell-based therapy in the treatment of a range of chronic, degenerative, and ischemic diseases.¹⁹ Benefits of MSC transplantation were demonstrated in clinical trials²⁰ and various animal experiments,^{21,22} but the underlying mechanisms remain elusive. With regard to the ischemic disease, it has been shown that transplantation of stem or progenitor cells can improve neovascularization and recovery of ischemic tissue and organ.^{23,24} The following four hypotheses currently ascribe this regenerative mechanisms to: (a) engraftment and differentiation of the administered cells into the cellular components of the host tissue or organ;^{23,25} (b) therapeutic fusion with the existing host cells;^{4,26–28} (c) release of paracrine signals from the administered cells;²⁹ and (d) stimulation of endogenous repair through the regeneration of stem cell niches in the local tissue.³⁰ The *in vitro* findings presented herein appeared to highlight an additional mechanism, that is, vasculogenic potential of MSC.

Focusing on the angiogenesis and ischemic disease, the data presented provide three independent lines of evidence demonstrating the angiogenic and vasculogenic potential of 4E cells: (1) *in vitro* transdifferentiation to endothelial-like and smooth muscle-like cells; (2) *in vivo* neovascularization of angioreactors; and (3) *in vivo* engraftment and transdifferentiation toward endothelial lineage after acute ischemic renal injury. Our data clearly demonstrate the propensity of MSC toward endothelial differentiation, as well as paracrine angiogenic chemoattraction.

It has been suggested previously that MSC may be one of the sources for circulating endothelial progenitor cells.^{4,31} Under certain conditions, they can also directly differentiate to endothelial cells.¹¹ Our previous data showed that 4E clone of MSC isolated from the kidney secrete angiogenic factors in culture and support endothelial cell growth and angiogenesis.⁸ Our *in vivo* angioreactor experiments with 4E cells are consistent with this notion, and hence support the paracrine mechanism of angiogenesis stimulated by MSC. Furthermore, our experiments also demonstrate an *in vivo* differentiation of 4E cells to the endothelial cells. In a sharp contrast to the rarely detected 4E cells when cultured in the growth factor-depleted matrigel, once VEGF-A/FGF-2 is present, 4E cells show signs of robust recruitment to and endothelial differentiation in the neovasculature. It is well-known that stem cell engraftment and endothelial differentiation are growth factor-dependent processes highly dependent on microenvironmental cues.³² This is further emphasized by the fact that in the absence of added growth factors to angioreactors, multiple capillaries are formed in spite of only sporadic incorporation of 4E cells into the functional neovessels (angiogenesis originating from the host vessels), whereas in the presence of growth factors 4E cells formed new vessels (vasculogenesis originating from implanted 4E cells).

In a previous study involving tumor angiogenesis, subcutaneous co-injection of bone marrow MSC with U-87 glioma cells in nude mice resulted in the formation of highly vascularized tumors.³³ In addition to the regulation through paracrine mechanism, it was documented that bone marrow MSC can be differentiated into CD31-positive cells, which constitute about 5% of the neovasculature of the solid tumor. Our experiments show that a significant proportion of 4E cells in the vicinity of the neovasculature were recruited into the vascular wall and differentiated into endothelial cells once VEGF/FGF was provided.

One of the characteristics of MSC is their ability to home to the sites of tissue damage or inflammation.³⁴ Using acute renal ischemia model, we observed significantly higher engraftment of the transplanted 4E cells in the ischemic kidney compared with the non-ischemic contralateral control at all tested time points over 1 month experimental period. These data support the concept that stem cell engraftment is highly dependent on local microenvironmental cues. Indeed, the 4E cells express CXCR4⁸ and upregulated renal SDF-1 signals after ischemic injury may have contributed to their preferential homing and engraftment. This ability of MSC to home to the sites of acute tissue injury has also been demonstrated in the settings of bone fracture,^{34,35} cerebral ischemia,³⁶ as well as the infarcted myocardium.³⁷

Because (a) there are no consistently reliable markers of these cells *in situ* and (b) a few available markers of these cells may disappear after cell differentiation, the strategy we elected was to isolate and expand clonal 4E MSC *ex vivo* and transfuse them *in vivo* as a surrogate for a behavior of the resident cells. Compared with the acquisition of endothelial lineage markers in both the *in vitro* cell culture and the *in vivo* angioreactor experiments, the endothelial transdifferentiation rate in our ischemic renal injury experiments is less robust: only 9% of the engrafted CM-DiI-labeled 4E cells in the ischemic kidney become Tie2-GFP-positive 30 days after transplantation, indicating their endothelial transdifferentiation. In comparison, the percentage of the engrafted 4E cells that become α SMA-positive 15–30 days after transplantation is higher. I/R injury can induce a wide range of gene expression including VEGF in the kidney.³⁸ These factors may orchestrate the observed 4E-to-endothelial or 4E-to-smooth muscle cell lineage transdifferentiation in the ischemic kidney. One could speculate that the composition of the post-ischemic microenvironment may be less favorable for 4E-to-endothelial transdifferentiation than the conditions found in our cell culture and angioreactor experiments. Nonetheless, the functional assessment of the ischemic kidney points out to the amelioration of renal dysfunction 2–3 days after ischemic episode by the 4E cell transplantation as judged by the plasma creatinine level. It is clear that the observed accelerated functional

improvement is unrelated to 4E cell transdifferentiation to the endothelial cells because the renoprotective effect occurs 24–48 h after 4E cell transplantation, as opposed to the much delayed transdifferentiation. One possible explanation for the early benefits of 4E cell delivery in the context of recovery from acute renal injury is the previously described paracrine mechanism.^{12,18,39} Indeed, 4E cell transplantation was associated with increased proliferation and reduced apoptosis of TECs. Moreover, microvascular rarefaction in the post-ischemic kidney was significantly reduced in the 4E-transplanted ischemic group, in synchrony with a fivefold increase in the renal expression of VEGF, in the absence of changes in systemic VEGF level. All this argues in favor of a local paracrine effect of 4E cell transplantation. In this regard, our data are in agreement with results obtained by Togel *et al.*¹⁸ On the other hand, the transdifferentiation potential toward the smooth muscle/myofibroblastic lineage may represent the mechanistic explanation for the long-term pro-fibrotic sequelae reported in renal ischemia.⁴⁰ It is quite possible that the proportion of MSC transdifferentiating toward the endothelial vs myofibroblastic lineage is an important determinant of the outcome of renal ischemia.

In summary, kidney-derived MSCs (4E cells) are vasculogenic as demonstrated by the analysis of implanted matrigel angioreactors supplemented with VEGF-A/FGF-2 growth factors. Despite this, in the context of acute ischemic injury, the transplantation of kidney-derived MSC (4E cell) affords renoprotection not through vasculogenesis, but rather through local paracrine effects that promote renal regeneration and prevent microvascular dropout.

MATERIALS AND METHODS

Animal studies

The animal study protocol was in accordance with the National Institutes of Health (NIH) Guide for the Care and Use of Laboratory Animals and approved by the Institutional Animal Care and Use Committee. Adult (8–20 weeks old) Tie-2/GFP mice⁴¹ (FVB/NJ strain) were purchased from The Jackson Laboratory (Bar Harbor, ME, USA). As the expression of GFP protein is under the control of Tie2 gene promoter/enhancer elements, it is hence present in virtually all endothelial cells where the Tie2 gene is constitutively expressed. This mouse model provided a convenient tool for monitoring the endothelial differentiation process. Animals were kept under temperature-controlled conditions of 12-h light/dark cycle, with water and food *ad libitum*. A separate group of mice was used as hosts of angiogenic cylinders (angioreactors) implanted subcutaneously as detailed below. Prior to the killing, mice were anesthetized with a combination of ketamine and xylazine and received intraperitoneal injection of 250 U/kg of heparin. Blood was collected from the left ventricle, and animals were flushed with 40 ml phosphate-buffered saline (PBS).

Isolation and culture of MSC–4E cells

Using a technique for culturing multipotent mesenchymal cells from adult tissues,^{1,42} we have previously isolated and cloned fibroblast-like cell line (referred to as 4E) from the kidney of adult Tie-2/GFP mouse. These 4E cells could be differentiated along multiple mesodermal lineages, including adipocytes, osteoblasts, as well as endothelial cells. Analysis of the expression of surface antigens, growth factor receptors, cytoskeletal proteins, and transcription factors revealed a pattern that was compatible with both mouse MSCs and renal stromal progenitor cells.⁸ 4E cells were maintained on gelatin-coated dishes in minimum essential medium (MEM) with 10% horse serum (Gem Biotech, Woodland, CA, USA) and consistently expressed the above markers between passages 10 and 25.

Flow cytometry analysis

Expression of GFP and staining of CD31 with phycoerythrin-conjugated antibody (BD Biosciences, Rockville, MD, USA) on the 4E cells following 1 month of three-dimensional

matrigel culture were measured using fluorescence-activated cell sorting as previously described.⁸ Each analysis included at least 10,000 events and was performed on at least two separate cell preparations.

***In vitro* angiogenesis assay**

Cultured 4E cells were detached with trypsin/EDTA, viable cells counted, and single-cell suspension (at a density of 2×10^5 cells per ml) was prepared using EGM-2 medium (Clonetics, San Diego, CA, USA) or MSC culture medium. A volume of 200 μ l per well of growth factor-depleted, phenol red-free Matrigel (BD Biosciences, San Jose, CA, USA) was plated in four-well chamber slides (BD Biosciences) and incubated at 37 °C for 15 min. The same volume (200 μ l) of cell suspension was plated on Matrigel. For comparison, the same amount of cells was also plated on chamber slides that were pre-coated overnight with fibronectin (BD Biosciences) at 4 °C. Endothelial capillary formation and the GFP signal were monitored using an inverted fluorescence microscope every 3 days over 1 month period. By the end of observations, the cells were washed with PBS and stained with phycoerythrin-labeled anti-mouse CD31 (PECAM-1, BD Biosciences) or α -SMA antibody (Dako North American, Carpinteria, CA, USA) with appropriate phycoerythrin-conjugated secondary antibody applied. After repeated washes with PBS, the chamber slides were examined and images obtained using Nikon fluorescent microscope (Eclipse TE2000-U) equipped with a digital camera (Spot model 4.2; Diagnostic Instruments, Sterling Heights, MI, USA).

***In vivo* angiogenesis and vasculogenesis studies using angioreactors**

The directed *in vivo* angiogenesis assay was adapted for our *in vivo* angiogenesis study. Matrigel filling and cylinder implantation procedure were conducted under sterile conditions following the previously published protocol⁴³ and the manufacturer's instructions (Trevigen Inc., Gaithersburg, MD, USA). In brief, the sterile implant-grade silicone cylinders, referred to as angioreactors, were filled at 4 °C with 20 μ l of matrigel containing FGF-2 (3.75 ng), VEGF-A (1.25 ng), and heparin (200 ng) with or without admixed 4E. The 4E cells were labeled with red fluorescent cell tracker CM-DiI (Molecular Probes, Eugene, OR, USA) and mixed with the matrigel at a density of 3000 cells per angioreactor. Cylinders were then incubated at 37 °C for 1 h to allow gel formation, and implanted subcutaneously into the dorsal flank of FVB mice. For each implantation experiment, four types of angioreactors were prepared: matrigel or growth factor alone, 4E/matrigel alone, and 4E/matrigel with VEGF-A/FGF-2. Fifteen days after implantation, angioreactors were harvested from the host mice. To visualize the ingrowth of the neovasculature from the host mice, 5 min before killing 100 μ l of LEL-FITC (1 mg/ml in 10 mM HEPES (4-(2-hydroxyethyl)-1-piperazineethanesulfonic acid), 150 mM NaCl, pH 7.5; Sigma, St Louis, MO, USA) was injected via tail vein to label the patent systemic vascular endothelium of the host mice. The collected angioreactors were fixed in 4% paraformaldehyde in PBS overnight at room temperature. The sealed bottom portion of the angioreactor was trimmed away with scissors. The fixed matrigel plugs were carefully removed. After washing with PBS, the gel plugs were whole mounted on chamber slides in glycerol/PBS and gently flattened under the coverslip. The slides were examined and images captured under a fluorescence microscope (Nikon) or confocal microscope (Zeiss Aniovert 200 inverted fluorescence microscope equipped with Zeiss Axiocam digital camera, Carl Zeiss, Hamburg, Mecklerburg, Germany) for deconvolution analysis. Z-stack images at 0.5 μ m per step were collected using $\times 10$ fluorescence objective lens and analyzed with Axiovision 4.4 software.

Transplantation of 4E cells in a model of renal ischemia

Unilateral or bilateral renal ischemia in male FVB/NJ mice (aged 8–20 weeks) was performed according to previously detailed protocol.⁸ Briefly, mice were anesthetized, a midline

laparotomy and bilateral or unilateral renal pedicle clamping was performed with microserrafines (Fine Science Tools, Foster City, CA, USA). The abdomen was covered with gauze moistened in PBS, and throughout the ischemia period, animals were kept well hydrated with saline and at a constant temperature (~37 °C) using a heated thermoplate (Tokai Hit, Fujinomiya-shi, Shizuoka-ken, Japan). After 30 min of ischemia, the clamps were removed, and reperfusion was confirmed visually. CM-DiI-labeled 4E cells (10^6 cells per animal) were injected intravenously via tail vein 24 h after reperfusion. Mice were killed at different time points between 1 and 30 days after renal I/R injury, blood samples were obtained and kidneys removed for further analyses. Plasma creatinine concentration was determined using a colorimetric assay (Cayman Chemical, Ann Arbor, MI, USA) according to the manufacturer's protocol.

Immunofluorescent and immunohistochemical analysis

Kidneys were fixed in 4% paraformaldehyde overnight at 4 °C, transferred to PBS containing 30% sucrose (overnight at 4 °C), embedded in OCT (Tissue Tek; Sakura Finetek, Torrance, CA, USA) and stored at -80 °C until analysis. Cryosections (10–20 μ m) were used for immunofluorescent and immunohistochemical analysis. The identification of engrafted transplanted 4E cells was done by detecting red fluorescent CM-DiI-labeled cells and the presence of GFP signal by fluorescence microscopy of kidney sections. To detect the expression of α SMA, sections were stained with mouse monoclonal anti- α SMA (1:250, Dako, Carpinteria, CA, USA), and tubular cell proliferation in the post-ischemic kidney was identified by staining sections with rabbit anti-Ki-67 polyclonal antibody (Abcam, Cambridge, MA, USA; 1:50). TUNEL assay using an In Situ Cell Death Detection Kit, TMR red (Roche, Indianapolis, IN, USA) was used to detect tubular cell apoptosis in post-ischemic kidney. Sections were screened for positive nuclei under a fluorescence microscope, and 20 random fields in the corticomedullary area were counted for every kidney at $\times 40$ magnification. Staining for peritubular capillary endothelial cells was performed on 20 μ m cryosections. Briefly, endogenous peroxidase activity and nonspecific binding were blocked, and sections were incubated overnight at 4 °C with rat anti-mouse CD31 antibody (MEC 13.3, BD Biosciences, 1:50), followed by incubation at room temperature with peroxidase-conjugated donkey anti-rat antibody (1:200, Jackson ImmunoResearch, West Grove, PA, USA) and chromogenic substrate 3,3'-diaminobenzidine (Dako). The sections were counter-stained with hematoxylin and mounted. Negative control received similar treatment with omission of the primary antibodies. Quantification of peritubular capillary loss was performed by calculating the rarefaction index as described.⁴⁴ The CD31-immunostained sections were examined through 10 \times 10 grid under a $\times 40$ objective. Each square within the grid that did not contain CD31-positive capillary was counted. At least 20 fields in the cortex and outer medulla were examined on the cross-section of each kidney, and a mean score per section was calculated. This scoring system, thus, inversely reflects peritubular capillary rarefaction, whereby low values represent intact capillaries and higher values indicate loss of capillaries (minimum possible capillary score is 0, and the maximum score is 100). The interstitial fibrosis was assessed with Masson's trichrome staining at low-power view ($\times 150$) and scored by an investigator blinded to the experimental design using a semi-quantitative scale (0, absent; 1, <25% of specimen area; 2, 25–50% of specimen area; 3, >50% of specimen area).

Renal tissue and plasma cytokine measurements

Snap-frozen decapsulated kidneys were lysed with RIPA buffer (1 \times PBS, 1% Nonidet P-40, 0.5% sodium deoxyolate, 0.1% SDS, and protease inhibitor), homogenized, and incubated at 4 °C for 30 min. Homogenates were subsequently centrifuged at 1500 g at 4 °C for 15 min, and supernatants and plasma were stored at -80 °C until assays were performed. Multiplexed cytokine measurements for renal tissue homogenates and plasma were performed using multiplex assay kit (MCYTO-70K-13, Millipore, St Charles, MO, USA), which allowed the

simultaneous quantification of the following analytes: TNF- α (Tumor Necrosis Factor α), Interleukin (IL)-1 α , IL- β , IL-6, KC, and IL-10. VEGF was measured using mouse single-plex VEGF Beadmates (46–196; Millipore). All analytes were tested individually and in combination to ensure that there were no cross-reactions. All measurements were performed in duplicate. The plates were analyzed using Luminex IS100 analyzer (Luminex Inc., Austin, TX, USA). The data were saved and evaluated as median fluorescence intensity (MFI) using appropriate curve-fitting software (Luminex 100IS software version 2.3). A five-parameter logistic method with weighting was used. Cytokine and VEGF levels were corrected for the amount of protein present using the Bio-Rad protein assay (Bio-Rad Laboratories, Hercules, CA, USA) with IgG as standard.

Statistical analysis

Data are expressed as mean \pm s.e.m. Differences between the groups were analyzed by analysis of variance or the Kruskal–Wallis test using SPSS 11.0 (SPSS, Chicago, IL, USA). A *P*-value less than 0.05 was considered statistically significant.

Acknowledgments

This study was supported by American Heart Association Scientist Development Grant 0430255N (J. Chen) and NIH Grants DK052783, DK45462, and DK054602 (M.S. Goligorsky). We are grateful to professor Michael Wolin and Dr. Qun Gao for their help with deconvolution image analysis.

References

1. da Silva Meirelles L, Chagastelles PC, Nardi NB. Mesenchymal stem cells reside in virtually all post-natal organs and tissues. *J Cell Sci* 2006;119:2204–2213. [PubMed: 16684817]
2. Kopp HG, Avezilla ST, Hooper AT, et al. The bone marrow vascular niche: home of HSC differentiation and mobilization. *Physiology (Bethesda)* 2005;20:349–356. [PubMed: 16174874]
3. Vaananen HK. Mesenchymal stem cells. *Ann Med* 2005;37:469–479. [PubMed: 16278160]
4. Jiang Y, Jahagirdar BN, Reinhardt RL, et al. Pluripotency of mesenchymal stem cells derived from adult marrow. *Nature* 2002;418:41–49. [PubMed: 12077603]
5. Patschan D, Plotkin M, Goligorsky MS. Therapeutic use of stem and endothelial progenitor cells in acute renal injury: ca ira. *Curr Opin Pharmacol* 2006;6:176–183. [PubMed: 16487748]
6. Silva GV, Litovsky S, Assad JA, et al. Mesenchymal stem cells differentiate into an endothelial phenotype, enhance vascular density, and improve heart function in a canine chronic ischemia model. *Circulation* 2005;111:150–156. [PubMed: 15642764]
7. Yin T, Li L. The stem cell niches in bone. *J Clin Invest* 2006;116:1195–1201. [PubMed: 16670760]
8. Plotkin MD, Goligorsky MS. Mesenchymal cells from adult kidney support angiogenesis and differentiate into multiple interstitial cell types including erythropoietin-producing fibroblasts. *Am J Physiol Renal Physiol* 2006;291:F902–F912. [PubMed: 16622175]
9. Ninichuk V, Gross O, Segerer S, et al. Multipotent mesenchymal stem cells reduce interstitial fibrosis but do not delay progression of chronic kidney disease in collagen4A3-deficient mice. *Kidney Int* 2006;70:121–129. [PubMed: 16723981]
10. Prodromidi EI, Poulosom R, Jeffery R, et al. Bone marrow-derived cells contribute to podocyte regeneration and amelioration of renal disease in a mouse model of Alport syndrome. *Stem Cells* 2006;24:2448–2455. [PubMed: 16873763]
11. Oswald J, Boxberger S, Jorgensen B, et al. Mesenchymal stem cells can be differentiated into endothelial cells *in vitro*. *Stem Cells* 2004;22:377–384. [PubMed: 15153614]
12. Togel F, Weiss K, Yang Y, et al. Vasculotropic, paracrine actions of infused mesenchymal stem cells are important to the recovery from acute kidney injury. *Am J Physiol Renal Physiol* 2007;292:F1626–F1635. [PubMed: 17213465]

13. Friedenstein AJ, Chailakhyan RK, Latsinik NV, et al. Stromal cells responsible for transferring the microenvironment of the hemopoietic tissues. Cloning *in vitro* and retransplantation *in vivo*. *Transplantation* 1974;17:331–340. [PubMed: 4150881]
14. Pereira RF, Halford KW, O'Hara MD, et al. Cultured adherent cells from marrow can serve as long-lasting precursor cells for bone, cartilage, and lung in irradiated mice. *Proc Natl Acad Sci USA* 1995;92:4857–4861. [PubMed: 7761413]
15. Pittenger MF, Mackay AM, Beck SC, et al. Multilineage potential of adult human mesenchymal stem cells. *Science* 1999;284:143–147. [PubMed: 10102814]
16. Reyes M, Verfaillie CM. Characterization of multipotent adult progenitor cells, a subpopulation of mesenchymal stem cells. *Ann N Y Acad Sci* 2001;938:231–235. [PubMed: 11458512]
17. Jiang Y, Vaessen B, Lenvik T, et al. Multipotent progenitor cells can be isolated from postnatal murine bone marrow, muscle, and brain. *Exp Hematol* 2002;30:896–904. [PubMed: 12160841]
18. Togel F, Hu Z, Weiss K, et al. Administered mesenchymal stem cells protect against ischemic acute renal failure through differentiation-independent mechanisms. *Am J Physiol Renal Physiol* 2005;289:F31–F42. [PubMed: 15713913]
19. Kassem M. Stem cells: potential therapy for age-related diseases. *Ann N Y Acad Sci* 2006;1067:436–442. [PubMed: 16804023]
20. Giordano A, Galderisi U, Marino IR. From the laboratory bench to the patient's bedside: an update on clinical trials with mesenchymal stem cells. *J Cell Physiol* 2007;211:27–35. [PubMed: 17226788]
21. Nagaya N, Kangawa K, Itoh T, et al. Transplantation of mesenchymal stem cells improves cardiac function in a rat model of dilated cardiomyopathy. *Circulation* 2005;112:1128–1135. [PubMed: 16103243]
22. Morigi M, Imberti B, Zoja C, et al. Mesenchymal stem cells are renotropic, helping to repair the kidney and improve function in acute renal failure. *J Am Soc Nephrol* 2004;15:1794–1804. [PubMed: 15213267]
23. Asahara T, Murohara T, Sullivan A, et al. Isolation of putative progenitor endothelial cells for angiogenesis. *Science* 1997;275:964–967. [PubMed: 9020076]
24. Kocher AA, Schuster MD, Szabolcs MJ, et al. Neovascularization of ischemic myocardium by human bone-marrow-derived angioblasts prevents cardiomyocyte apoptosis, reduces remodeling and improves cardiac function. *Nat Med* 2001;7:430–436. [PubMed: 11283669]
25. Kalka C, Masuda H, Takahashi T, et al. Transplantation of *ex vivo* expanded endothelial progenitor cells for therapeutic neovascularization. *Proc Natl Acad Sci USA* 2000;97:3422–3427. [PubMed: 10725398]
26. Terada N, Hamazaki T, Oka M, et al. Bone marrow cells adopt the phenotype of other cells by spontaneous cell fusion. *Nature* 2002;416:542–545. [PubMed: 11932747]
27. Ying QL, Nichols J, Evans EP, et al. Changing potency by spontaneous fusion. *Nature* 2002;416:545–548. [PubMed: 11932748]
28. Alvarez-Dolado M, Pardal R, Garcia-Verdugo JM, et al. Fusion of bone-marrow-derived cells with Purkinje neurons, cardiomyocytes and hepatocytes. *Nature* 2003;425:968–973. [PubMed: 14555960]
29. Kinnaird T, Stabile E, Burnett MS, et al. Marrow-derived stromal cells express genes encoding a broad spectrum of arteriogenic cytokines and promote *in vitro* and *in vivo* arteriogenesis through paracrine mechanisms. *Circ Res* 2004;94:678–685. [PubMed: 14739163]
30. Mazhari R, Hare JM. Mechanisms of action of mesenchymal stem cells in cardiac repair: potential influences on the cardiac stem cell niche. *Nat Clin Pract Cardiovasc Med* 2007;4:S21–S26. [PubMed: 17230212]
31. Reyes M, Dudek A, Jahagirdar B, et al. Origin of endothelial progenitors in human postnatal bone marrow. *J Clin Invest* 2002;109:337–346. [PubMed: 11827993]
32. Aghi M, Cohen KS, Klein RJ, et al. Tumor stromal-derived factor-1 recruits vascular progenitors to mitotic neovasculature, where microenvironment influences their differentiated phenotypes. *Cancer Res* 2006;66:9054–9064. [PubMed: 16982747]
33. Annabi B, Naud E, Lee YT, et al. Vascular progenitors derived from murine bone marrow stromal cells are regulated by fibroblast growth factor and are avidly recruited by vascularizing tumors. *J Cell Biochem* 2004;91:1146–1158. [PubMed: 15048870]

34. Devine SM, Bartholomew AM, Mahmud N, et al. Mesenchymal stem cells are capable of homing to the bone marrow of non-human primates following systemic infusion. *Exp Hematol* 2001;29:244–255. [PubMed: 11166464]
35. Devine MJ, Mierisch CM, Jang E, et al. Transplanted bone marrow cells localize to fracture callus in a mouse model. *J Orthop Res* 2002;20:1232–1239. [PubMed: 12472234]
36. Wang L, Li Y, Chen J, et al. Ischemic cerebral tissue and MCP-1 enhance rat bone marrow stromal cell migration in interface culture. *Exp Hematol* 2002;30:831–836. [PubMed: 12135683]
37. Price MJ, Chou CC, Frantzen M, et al. Intravenous mesenchymal stem cell therapy early after reperfused acute myocardial infarction improves left ventricular function and alters electrophysiologic properties. *Int J Cardiol* 2006;111:231–239. [PubMed: 16246440]
38. Villanueva S, Cespedes C, Vio CP. Ischemic acute renal failure induces the expression of a wide range of nephrogenic proteins. *Am J Physiol Regul Integr Comp Physiol* 2006;290:R861–R870. [PubMed: 16284088]
39. Hung SC, Pochampally RR, Chen SC, et al. Angiogenic effects of human multipotent stromal cell conditioned medium activate the PI3K–Akt pathway in hypoxic endothelial cells to inhibit apoptosis, increase survival, and stimulate angiogenesis. *Stem Cells* 2007;25:2363–2370. [PubMed: 17540857]
40. Basile DP. The endothelial cell in ischemic acute kidney injury: implications for acute and chronic function. *Kidney Int* 2007;72:151–156. [PubMed: 17495858]
41. Motoike T, Loughna S, Perens E, et al. Universal GFP reporter for the study of vascular development. *Genesis* 2000;28:75–81. [PubMed: 11064424]
42. Lucas PA, Calcutt AF, Southerland SS, et al. A population of cells resident within embryonic and newborn rat skeletal muscle is capable of differentiating into multiple mesodermal phenotypes. *Wound Repair Regen* 1995;3:449–460. [PubMed: 17147656]
43. Guedez L, Rivera AM, Salloum R, et al. Quantitative assessment of angiogenic responses by the directed *in vivo* angiogenesis assay. *Am J Pathol* 2003;162:1431–1439. [PubMed: 12707026]
44. Gerber HP, Hillan KJ, Ryan AM, et al. VEGF is required for growth and survival in neonatal mice. *Development* 1999;126:1149–1159. [PubMed: 10021335]

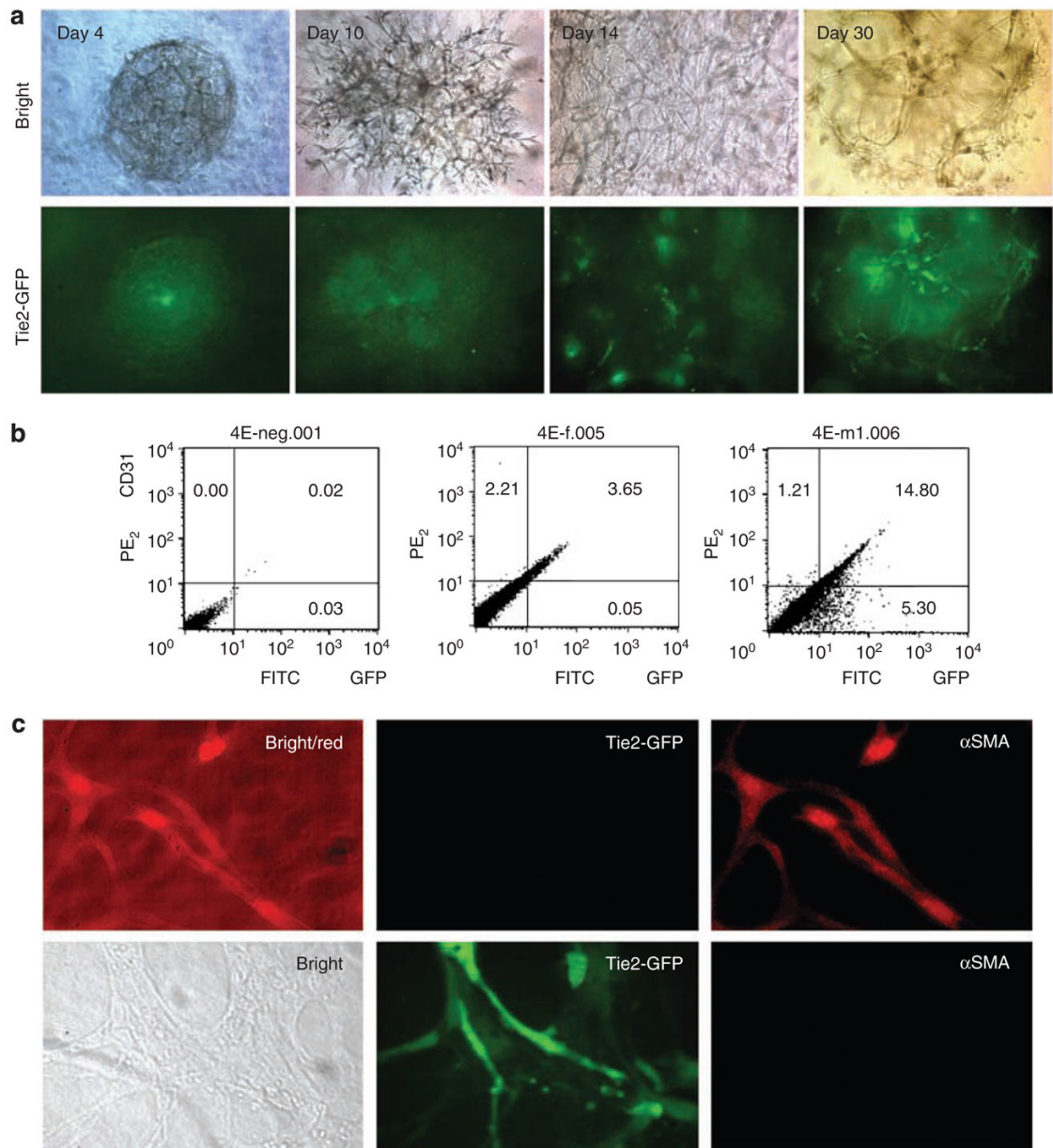


Figure 1. *In vitro* differentiation of 4E cells into endothelial- and smooth muscle-like cells
(a) The 4E initially formed 'sphere'-like structure that gradually spread out forming numerous capillaries. Acquisition of GFP + signal by these cells and their morphology are illustrated.
(b) FACS analysis of 4E cells maintained in MSC culture medium showed the absence of GFP/CD31 double-positive cells, further confirming that these cells initially did not contain endothelial cells (left panel). However, when 4E cells were cultured for 30 days in matrigel/EGM-2 medium, 14.8% cells were GFP/CD31 double-positive (right panel), whereas only 3.65% became double positive in fibronectin/EGM-2 medium (middle panel). **(c)** The 4E cells differentiated into smooth muscle-like cells expressing α SMA, but not Tie2-GFP, when cultured in MSC medium (upper panel). In contrast, 4E cells differentiated into endothelial-like cells expressing Tie2-GFP, but not α SMA, when cultured on matrigel in EGM-2 medium (c).

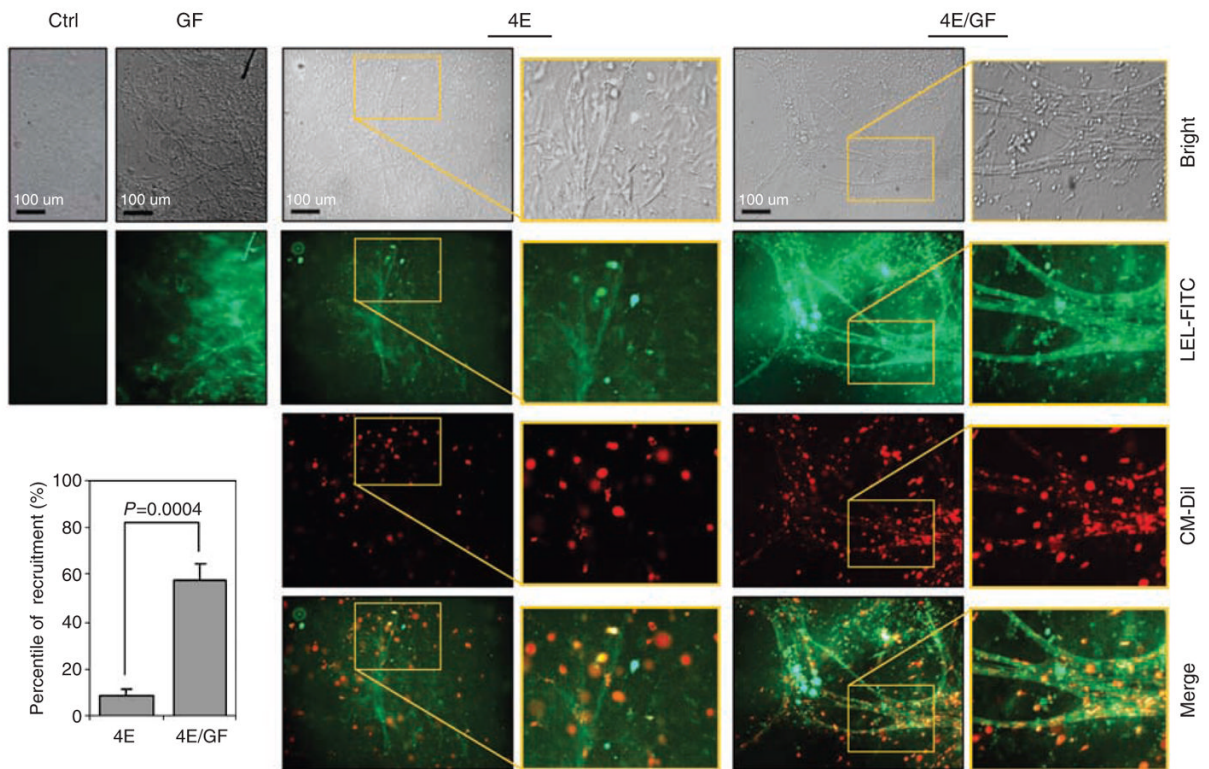


Figure 2. *In vivo* contribution of 4E cells to neovascularization of angioreactors

Fifteen days after subcutaneous implantation of angioreactors, 4E cells promoted the invasion of endothelial cell ingrowth into the matrigel. The neovasculature appears functional as vessels are lectin-FITC-positive. With the addition of VEGF/FGF, the functional neovasculature showed signs of more vigorous growth and mature architecture, and the engraftment of 4E into the vascular wall was dramatically enhanced. Many of the engrafting 4E cells were green fluorescence-positive, reflecting their endothelial differentiation indicated by either one or both of the events, the expression of Tie2-GFP or/and *Lycopersicon Esculentum* lectin-FITC (LEL-FITC) staining. The high-magnification images are inserted on the right panel and show the framed area. Growth factor (GF)-depleted matrigel alone did not support any visible invasion of endothelial cells or ingrowth of capillaries. The 4E cells were pre-labeled with cell tracker CM-DiI (red fluorescence).

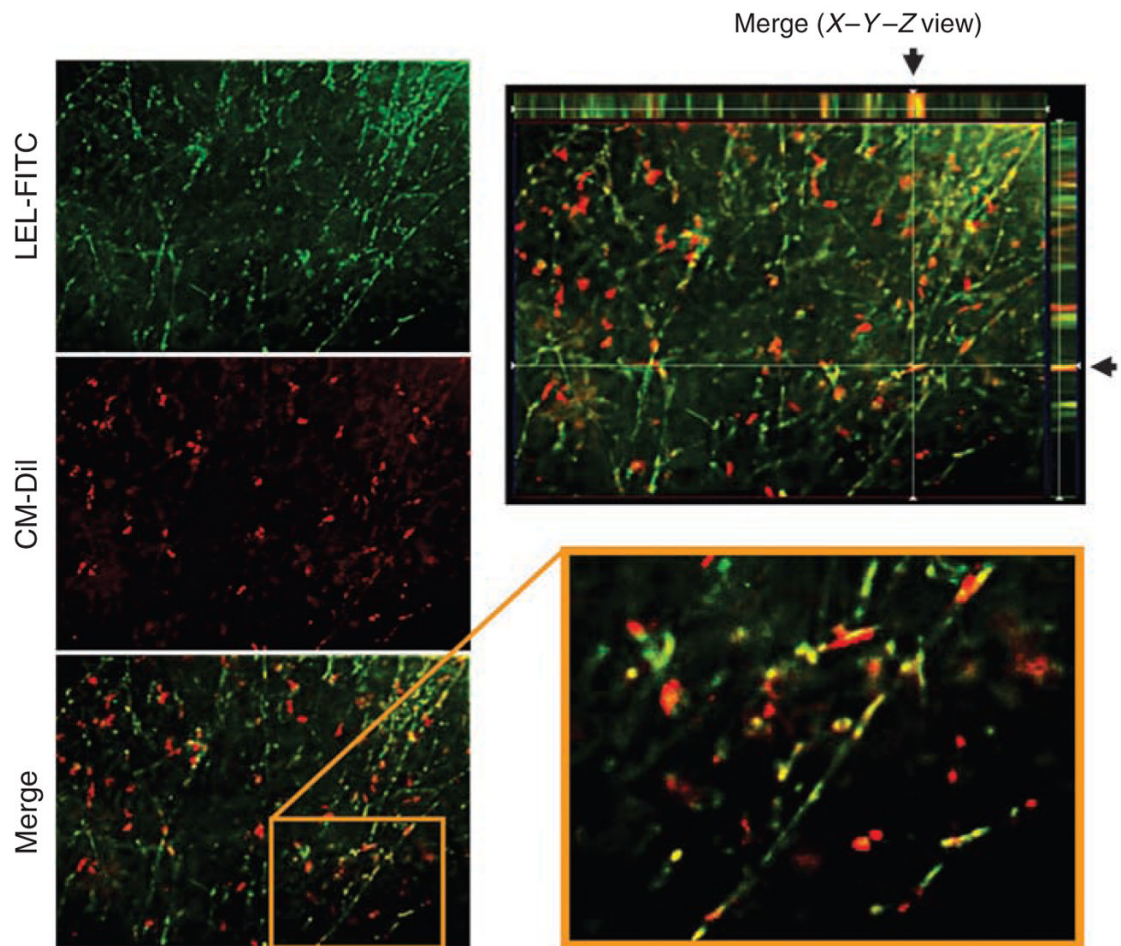


Figure 3. *In vivo* contribution of 4E cells to neovascularization

To better visualize the participation of 4E cells in the neovascularization, angioreactors were also analyzed using deconvolution microscopy. Images on the left represent consecutive fluorescence microscopy of the LEL-FITC and CM-Dil-labeled cells as well as the merged image. The image on the right (top panel) shows a three-dimensional reconstruction of the angioreactor, representing stacks of frames spanning 40 μm in thickness. The double-positive cell in the cross of the vertical and horizontal lines is indicated by the arrows in the cross-sectional X- and Y-view strips. The image in the lower right panel shows an enlarged area framed in the merged image.

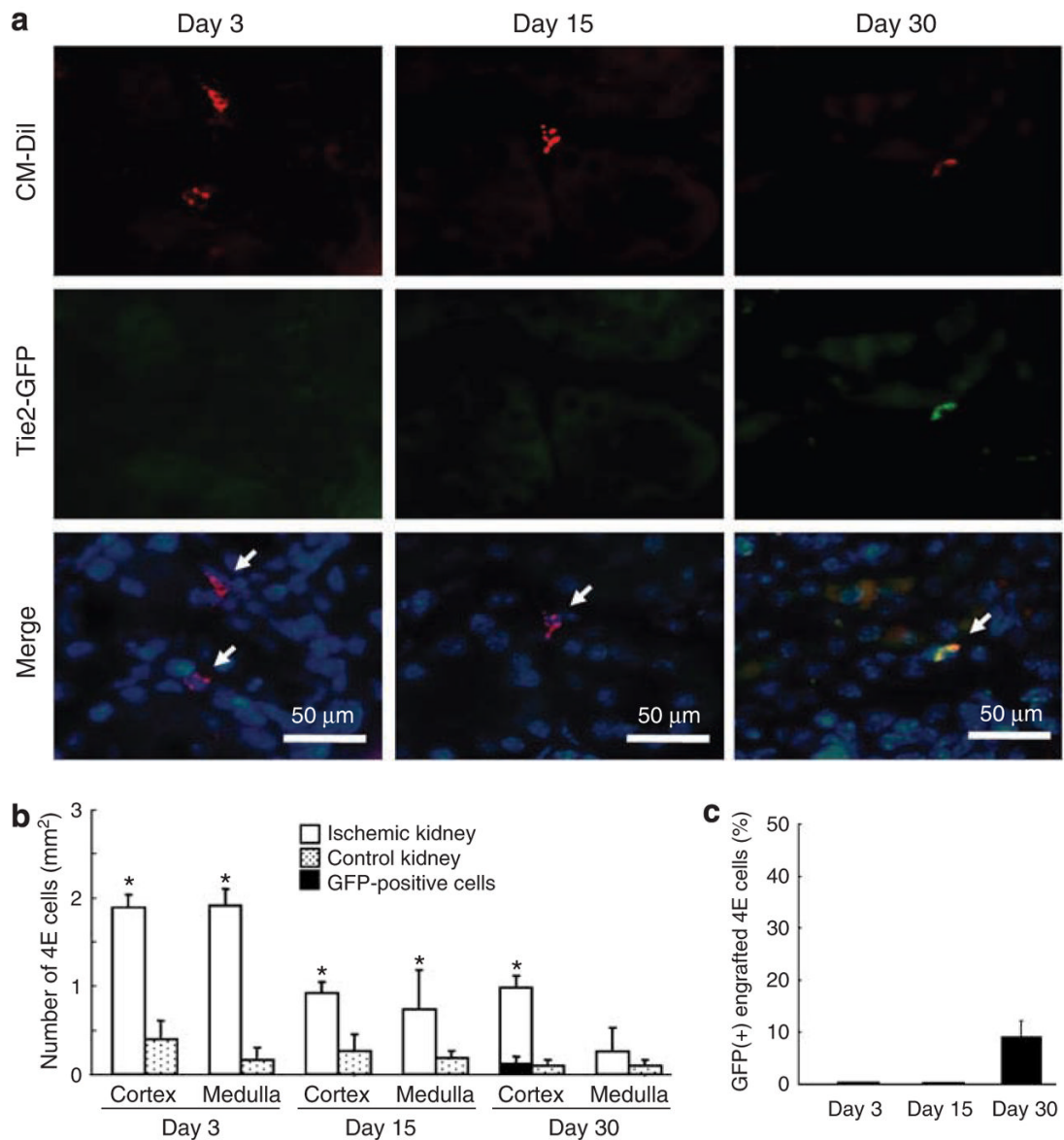


Figure 4. Analysis of the engraftment and transdifferentiation of transplanted 4E cells after I/R injury

The number of engrafted CM-DiI-labeled 4E cells in peritubular capillaries of the unilateral ischemic kidney was compared with the contralateral non-ischemic control 3, 15, and 30 days after I/R injury. **(a)** Representative images of red fluorescent CM-DiI-labeled 4E cells (arrow) and Tie2-GFP fluorescence of kidneys at different times after ischemia. **(b)** The summary of quantitative analysis of engrafted cells and the appearance of GFP fluorescence. **(c)** After 30 days, $9.2 \pm 3.1\%$ of the engrafted CM-DiI-labeled cells become Tie2-GFP-positive. Arrows indicate CM-DiI- and/or GFP-expressing cells. Nuclei were stained with DAPI. Original magnification was $\times 600$. $*P < 0.05$ vs control. $n = 6$ mice for each group, values are mean \pm s.e.m.

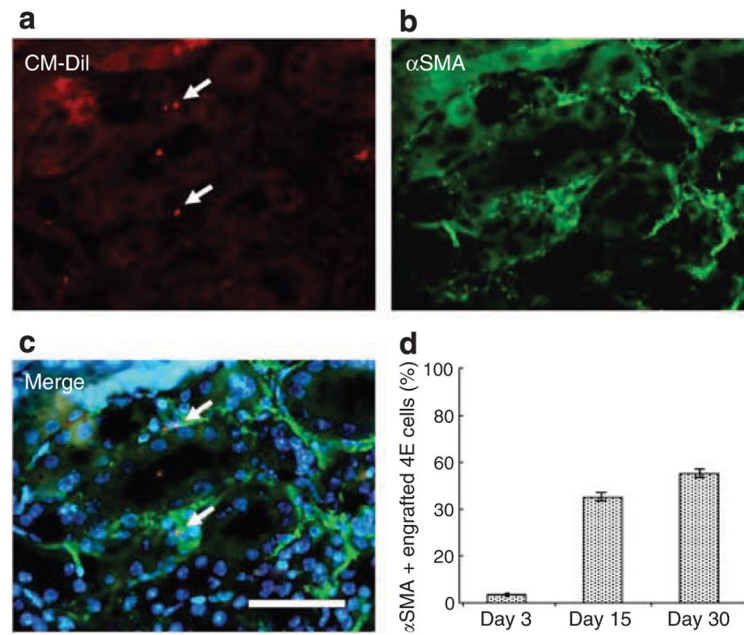


Figure 5. Immunofluorescence analysis of the expression of α SMA in engrafted 4E cells in ischemic kidney

(a–c) Representative images of CM-Dil- and/or α SMA-expressing 4E cell engrafting ischemic kidneys (merged image shown in panel c with the nuclear DAPI staining) 30 days after I/R injury. (d) Quantitative analysis of results at 3–30 days after I/R injury. Original magnification was $\times 400$. $*P < 0.01$ vs 3 days. $n = 4$ in each group, values are mean \pm s.e.m.

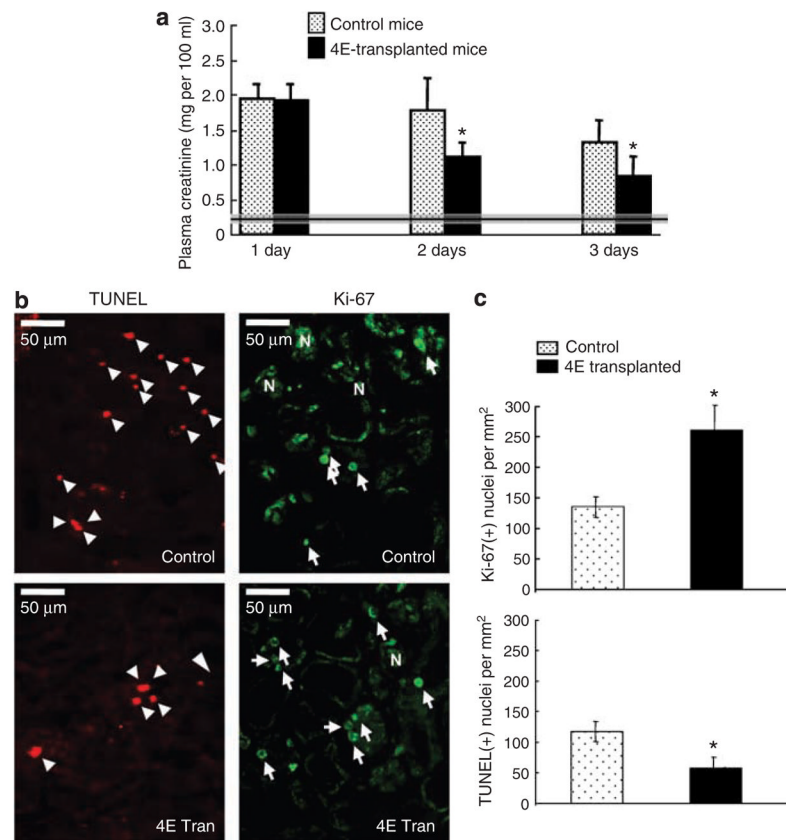


Figure 6. Accelerated renal functional recovery by 4E cell transplantation after I/R injury

(a) The measurement of plasma creatinine concentration demonstrated a significantly lower creatinine level in transplanted mice 2–3 days after I/R renal injury. The shaded line shows the baseline plasma creatinine level in normal mice (0.24 ± 0.07 mg per 100 ml). (b) Representative images of Ki-67 and TUNEL stainings in control and 4E-transplanted mouse kidneys. (c) Quantitative analysis of Ki-67 and TUNEL-positive cells in the kidney sections 3 days after ischemic injury. Original magnification was $\times 400$. $*P < 0.05$ vs non-transplanted control mice with I/R injury, *N*, area of necrosis. $n = 6$ in each group, values are mean \pm s.e.m.

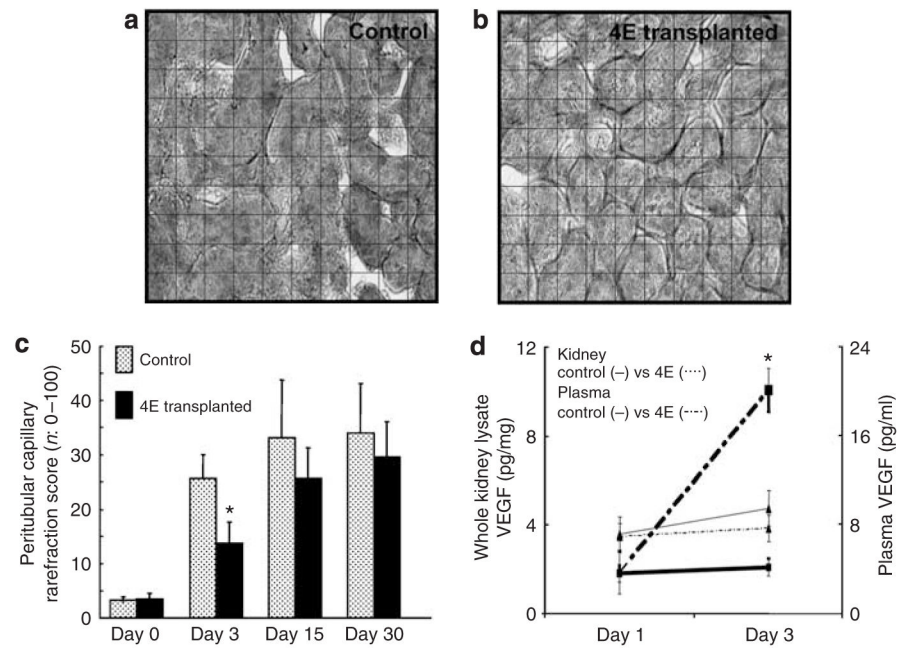


Figure 7. Microvascular rarefaction in post-ischemic kidneys

Representative images of CD31 staining in control (a) and 4E-injected (b) mice on day 3 after I/R injury. (c) To quantify vascular dropout in post-ischemic kidneys, microvascular rarefaction index was calculated as detailed in Materials and Methods. Three days post-ischemia microvasculature was significantly preserved by the administration of 4E cells compared with un-treated kidneys. At later times, 15 and 30 days post-ischemia, the differences in rarefaction index disappeared. (d) 4E-Transplanted mouse kidneys showed a fivefold increase in renal VEGF expression at 3 days after I/R injury. In contrast, plasma VEGF level did not show any significant difference between the two groups. Original magnification was $\times 400$. * $P < 0.05$ vs control. $n = 4$ in each group, values are mean \pm s.e.m.